© 2023. Published by The Company of Biologists Ltd | Journal of Experimental Biology (2023) 226, jeb245973. doi:10.1242/jeb.245973

RESEARCH ARTICLE

Comparison of auditory evoked potential thresholds in three shark species

Carolin Nieder*, Jimmy Rapson, John C. Montgomery and Craig A. Radford

ABSTRACT

Auditory sensitivity measurements have been published for only 12 of the more than 1150 extant species of elasmobranchs (sharks, skates and rays). Thus, there is a need to further understand sound perception in more species from different ecological niches. In this study, the auditory evoked potential (AEP) technique was used to compare hearing abilities of the bottom-dwelling New Zealand carpet shark (*Cephaloscyllium isabellum*) and two benthopelagic houndsharks (Triakidae), the rig (*Mustelus lenticulatus*) and the school shark (*Galeorhinus galeus*). AEPs were measured in response to tone bursts (frequencies: 80, 100, 150, 200, 300, 450, 600, 800 and 1200 Hz) from an underwater speaker positioned 55 cm in front of the shark in an experimental tank. AEP detection thresholds were derived visually and statistically, with statistical measures slightly more sensitive (∼4 dB) than visual methodology. Hearing abilities differed between species, mainly with respect to bandwidth rather than sensitivity. Hearing was least developed in the benthic *C. isabellum* [upper limit: 300 Hz, highest sensitivity: 100 Hz (82.3 ±1.5 dB re. 1 µm s^{-2})] and had a wider range in the benthopelagic rig and school sharks [upper limit: 800 Hz; highest sensitivity: 100 Hz (79.2±1.6 dB re. 1 µm s^{-2}) for *G. galeus* and 150 Hz (74.8±1.8 dB re. 1 µm s^{-2}) for *M. lenticulatus*]. The data are consistent with those known for 'hearing non-specialist' teleost fishes that detect only particle motion, not pressure. Furthermore, our results provide evidence that benthopelagic sharks exploit higher frequencies (max. 800 Hz) than some of the bottom-dwelling sharks (max. 300 Hz). Further behavioural and morphological studies are needed to identify what ecological factors drive differences in upper frequency limits of hearing in elasmobranchs.

KEY WORDS: Elasmobranchs, Hearing sensitivity, Electrophysiology, New Zealand carpet shark, *Cephaloscyllium isabellum*, Rig shark, *Mustelus lenticulatus*, School shark, *Galeorhinus galeus*

INTRODUCTION

Elasmobranchs (sharks, skates, and rays) are generally regarded as having a poor sense of hearing. This perception is based upon the relatively poor acoustic sensitivity and narrow frequency detection bandwidth (<1 kHz) compared with most teleosts (Maisey and Lane, 2010; Popper et al., 2021). Auditory research in elasmobranchs has received little attention, with basic acoustic sensitivity measurements published for only 12 of the more than 1150 extant species of elasmobranch (Chapuis and Collin, 2022; Ebert et al., 2021; Wiernicki et al., 2020). Yet, sound may be of greater importance to this ancient and diverse group of fishes than previously thought. Behavioural evidence suggests that elasmobranchs use sound for prey detection (Backus, 1963; Banner, 1972; Myrberg, 1972; Myrberg et al., 1976; Nelson and Gruber, 1963; Nelson and Johnson, 1972; Richard, 1968), predator avoidance (Chapuis et al., 2019; Fetterplace et al., 2022; Klimley and Myrberg, 1979; Myrberg et al., 1978) and potentially also reproduction (Carrier, Pratt, and Martin, 1994). Despite the behavioural evidence, there is relatively little physiological data on understanding sound perception in elasmobranchs and their close relatives (Chapuis and Collin, 2022; Mickle and Higgs, 2022).

Underwater sound consists of two components: sound pressure, which is a scalar and omnidirectional, and particle motion, which is a vector and directional (Rogers and Cox, 1988). In fish, the lateral line and the inner ear detect particle motion (Kalmijn, 1988). The ear has three semi-circular canals that are involved in determining the angular movements of the fish (Lowenstein, 1971). The ear also has three otoconial organs, the saccule, lagena and utricle, that are involved in both determining the orientation of the fish relative to gravity and detecting sound (Lowenstein and Roberts, 1950, 1951; Corwin, 1981b; Kalmijn, 1988; Popper and Fay, 1977). The otoconial endorgans contain sensory epithelia (maculae) composed of supporting cells and sensory hair cells that are overlaid with a dense otoconial mass (Mulligan and Gauldie, 1989) (Mulligan and Gauldie, 1989; Tester et al., 1972). At the apical ends of the hair cells are ciliary bundles, composed of many stereocilia that are organized in a stepwise arrangement of increasing height, leading to a single kinocilium (Flock, 1971). The vibrations generated by a sound source efficiently propagate through the water and move the fish as water and fish have similar densities (Rogers and Cox, 1988). The denser otoconia lag the motions of surrounding soft tissue and bend the hair cell bundles, which activates the auditory system (Flock and Wersall, 1963). Fishes with internal gas-filled structures (e.g. swim bladder, auditory bullae, branchial bubbles) can detect sound pressure (Popper and Fay, 1977). The vibrations of the gas bubble transform the pressure signal into particle motion, which is then transmitted to the inner ear (Sand and Enger, 1973). Elasmobranchs lack any known pressure-transducing structure; therefore, it is thought that they can only detect the particle motion component of the sound field (Banner, 1967; Kelly and Nelson, 1975; Popper and Hawkins, 2021).

Elasmobranchs also detect sound using a fourth endorgan that is not loaded with an otoconial mass, the macula neglecta, located inside the posterior canal duct (Corwin, 1977, 1981b; Fay et al., 1974; Lowenstein and Roberts, 1951; Retzius, 1881). The macula neglecta is particularly well developed in sharks and is thought to function in directional hearing in carcharhinid sharks (Corwin, 1977, 1978). The hair cells are embedded in a gelatinous cupula,

Institute of Marine Science, University of Auckland, Leigh Marine Research Laboratory, Leigh, Auckland 0985, New Zealand.

*Author for correspondence (cnie398@aucklanduni.ac.nz)

C.N., 0000-0001-5719-1352; J.C.M., 0000-0002-7451-3541; C.A.R., 0000-0001-7949-9497

Received 17 April 2023; Accepted 4 July 2023

Journal of Experimental Biology (2023) 226, jeb245973. doi:10.1242/jeb.245973

which is suspended in the endolymphatic fluid of the posterior canal duct (Tester et al., 1972). The hair cells of the macula neglecta are very likely stimulated by movements of the cupula (Tester et al., 1972); however, the modus operandi, including the adequate stimulus have not been unequivocally demonstrated (Popper and Fay, 2011).

Regardless of the mechanism, when bent in the appropriate direction, the sensory hair cells of the otoconial endorgans and the macula neglecta, convert acoustic energy into electric potentials that can be measured from the eighth nerve and higher auditory centres in the brainstem (Bullock and Corwin, 1979; Fay and Popper, 2000; Flock and Wersall, 1963). The auditory evoked potential (AEP) technique has commonly been used to measure basic acoustic abilities in fish (Ladich and Fay, 2013), including sharks (Bullock and Corwin, 1979; Casper and Mann, 2009; Corwin et al., 1982). It is a relatively quick, non-invasive method to record compound field potentials of the entire auditory system (Bullock and Corwin, 1979; Corwin et al., 1982; Kenyon et al., 1998). The method has its limitations, because hearing is a complex cognitive process that requires signal integration at the level of the whole animal and the AEP technique only represents one part of that (Popper et al., 2019; Popper and Hawkins, 2021). Nonetheless, the AEP technique has proven extremely useful to compare frequency detection range and best sensitivity among different species (Ladich and Fay, 2013; Vetter et al., 2018; Wysocki et al., 2009a). A review of AEP-generated detection threshold curves includes only two species of ray and six shark species (Ladich and Fay, 2013), highlighting the need to assess more species from different families, habitats and ecological roles.

The goal of this study was to measure auditory detection thresholds in the New Zealand carpet shark (*Cephaloscyllium isabellum*), the rig shark (*Mustelus lenticulatus*) and the school shark (*Galeorhinus galeus*) using the AEP technique in combination with an underwater speaker tank setup. The carpet shark is a nocturnal slow-swimming benthic shark. The benthopelagic rig shark swims most of the time and specialises in crushing crustaceans close to the seafloor (Francis et al., 2012). The school shark is a benthopelagic species that continuously swims and preys on small fishes and invertebrates (Francis and Mulligan, 1998). The results of the present study extend current knowledge of elasmobranch hearing abilities and will be useful for future integration with morphological and behavioural studies.

MATERIALS AND METHODS

Animal collection and husbandry

Six rig sharks (*Mustelus lenticulatus* Phillipps 1932) (3 male, 3 female; TL range 51.5–70 cm) and seven school sharks (*Galeorhinus galeus* Linnaeus 1758) (4 male, 3 female; TL range 49.5–75 cm) were caught using circle-hook and line in the Kaipara Harbour (New Zealand, North Island). Eight carpet sharks (*Cephaloscyllium isabellum* Bonnaterre 1788) (5 male, 3 female; TL range 58.5–75 cm) were obtained from local commercial fishermen (Table 1). Animals were housed in flow-through holding tanks, supplied with ambient seawater, and maintained on a mixed diet of squid and fish three times a week. Sharks were acclimated for at least 1 week prior to experimentation. All procedures were conducted in accordance with ethics protocols #002066/#AEC23071, approved by the University of Auckland Animal Ethics Committee (AEC).

Table 1. Sharks used for AEP measurements with an underwater speaker

	Sex	Total length (cm)	Age class
Carpet shark (*Cephaloscyllium isabellum*)			
T-CS5	Male	58.5	Juvenile
T-CS3	Male	63.5	Adult
T-CS9	Male	62.8	Adult
T-CS1	Male	65.0	Adult
T-CS8	Male	67.0	Adult
T-CS7	Female	70.0	Juvenile
T-CS6	Female	70.5	Juvenile
T-CS4	Female	75.0	Juvenile
Rig shark (*Mustelus lenticulatus*)			
T-Rig6	Male	51.5	Juvenile
T-Rig5	Male	53.5	Juvenile
T-Rig9	Male	56.8	Juvenile
T-Rig7	Female	62.0	Juvenile
T-Rig8	Female	67.0	Juvenile
T-Rig10	Female	70.0	Juvenile
School shark (*Galeorhinus galeus*)			
T-School3	Male	49.5	Juvenile
T-School1	Male	51.3	Juvenile
T-School5	Male	58.5	Juvenile
T-School7	Male	63.5	Juvenile
T-School4	Female	58.0	Juvenile
T-School6	Female	72.5	Juvenile
T-School2	Female	73.5	Juvenile

Age class was assigned based on the average total length (TL) at maturity published for the carpet shark [male, ∼60 cm; female, ∼75 cm (Horn, 2016)], rig shark [male, ∼85 cm; female, ∼100 cm (Francis and Francis, 1992)], and school shark [male, ∼125–135 cm; female, ∼135–140 cm (Francis and Mulligan, 1998)].

Tank setup, stimulus generation

A 4360 litre circular tank (made of high-density polyethylene, 2100 mm inside diameter, 1260 mm water depth) was isolated from ground vibrations by sitting it on rubber tyres. A monopole underwater loudspeaker (UW-30, Lubell Labs Inc., Columbus, OH, USA) was wrapped in aluminium foil and grounded to reduce signal interference during AEP recordings. The speaker was suspended from a wooden plank using nylon and bungee cords and positioned in the centre of the tank 65 cm below the surface (Fig. 1). The plank was isolated from the tank with multiple sheets of vibration- and noise-dampening mats. The water temperature and salinity ranged from 14.7 to 22.5°C and 35–36 ppt, respectively.

Auditory stimuli were produced by a sound module (Tucker-Davis Technologies, TDT, Gainesville, FL, USA) operated by a laptop (Lenovo ThinkPad X270) running SigGen® (v. 4.4.9) and BioSig® (v. 4.4.11) software. Signals were digitised (RP 2.1, TDT) attenuated (PA5, TDT) and amplified (Pyle®, PLA2378, Sonic Electronix, Louisville, KY USA) before being played through the speaker. Auditory signals consisted of pulsed tone bursts (25–50 ms duration, with a 3 ms rise/fall time gated through a Hanning window) at 80, 100, 150, 200, 300, 450, 600, 800 and 1200 Hz (Table 2). The frequency specificity of acoustic tone pips in confined tank setups can depend on the stimulus duration (e.g. Christensen et al., 2015; Lauridsen et al., 2021). Initial examinations of the frequency spectra of all test stimuli in our tank setup revealed that optimal frequency specificity was achieved for pip durations of 50 ms for the lower frequency tone-bursts (<450 Hz), and 25 ms for frequencies 450–1200 Hz. Pressure waveforms, spectral levels and particle acceleration magnitude spectra are shown in Fig. 2.

Acoustic evoked potential measurements

Prior to experiments the shark was anesthetized by immersion (∼10–15 min) in a salt-water bath of MS-222 (ethyl 3-aminobenzoate

Journal of Experimental Biology (2023) 226, jeb245973. doi:10.1242/jeb.245973

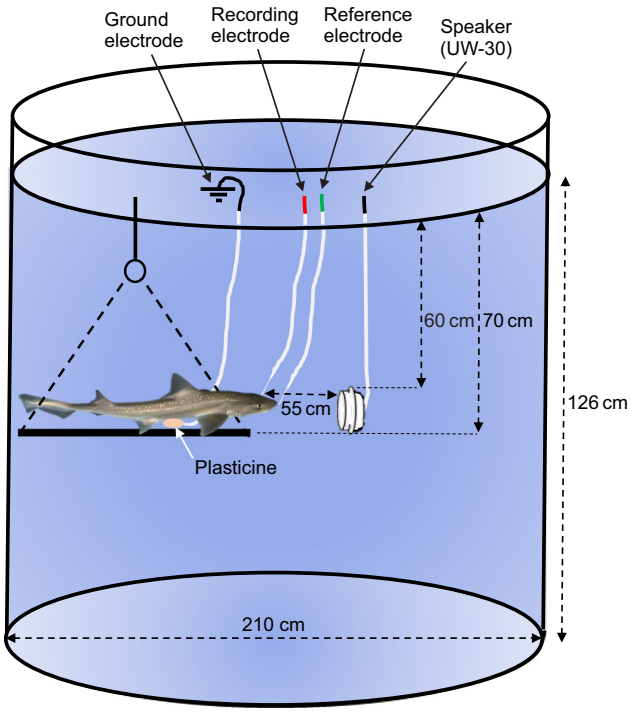

Fig. 1. Experimental tank setup. The shark was attached to a custom-made plastic mesh holder (not shown) and suspended ~70 cm below the waterline, such that the inner ear of the shark was positioned 55 cm in front and 5 cm above the underwater loudspeaker. The recording electrode (red) was inserted dorsally, underneath the skin, at the border of the parietal fossa, where it has its widest (medial-lateral) diameter. The reference electrode (green) was inserted into the cartilage at the tip of the snout, and the ground electrode (black) was placed in Plasticine next to the shark's body. The underwater speaker and electrode wires were wrapped in foil and grounded to shield them from electrical noise.

methanesulfonate, PubChem Substance ID: 24894382, Sigma Aldrich) and sodium hydrogen bicarbonate in a 1:2 ratio. When there was no response to tail-pinching, the shark was firmly wrapped (from pectoral fins to tail, leaving the gills exposed for breathing to occur normally) into a piece of stocking, and positioned ventrally onto a custom-made plastic mesh holder, where it was secured with Velcro straps. Stainless steel reusable subdermal needle electrodes (27 gauge, 13 mm, Rochester Electromedical Inc.; Coral Springs, FL, USA) were used to record AEPs. The recording electrode was inserted dorsally, underneath the skin, at the border of the largest lateral-medial diameter of the parietal fossa. The reference electrode was inserted into the cartilage at the tip of the snout, and the ground electrode was placed in plasticine next to the shark's body. The electrodes were insulated with nail varnish, apart from the tips. The electrode wires were tightly wrapped in foil tape and surrounded by a grounded stainless steel mesh sleeve to minimise interference and electrical noise.

The animal holder was then carefully lowered into the tank to ~70 cm under the waterline, such that the inner ear of the shark was positioned 55 cm in front, and 5 cm above the underwater speaker (Fig. 1). Carpet and rig sharks are buccal pumpers, therefore were allowed to recover from the initial anaesthesia. School sharks are ram ventilators and therefore needed to be ventilated with a dilute mixture of anaesthetic (0.075 g L^{-1} MS-222 and 0.115 g L^{-1} sodium hydrogen bicarbonate) that was dripped through the mouth and over the gills during the experiment to maintain a mild anaesthetised state. Previous research (Chapius et al., 2019) has shown that MS222 has no significant effect on the shark's AEP responses at the concentrations used in this study. The presentation order of the frequencies was conducted randomly. An average of 1200 responses (600 sweeps from stimuli presented at 0 deg and 600 sweeps from stimuli presented at 180 deg) was taken for each sound pressure level (SPL) at each frequency. However, to verify AEPs close to threshold level 2000 sweeps were undertaken (e.g. 1000 sweeps at each polarity). AEPs were first elicited using a SPL above threshold (Table 2). The SPLs were then decreased in 5 dB steps for each frequency until an AEP could no longer be visually identified. Then, one to three additional measurements, at 5–15 dB below this roughly estimated threshold were made to ensure responses were not missed. The presence of an AEP was verified visually through (1) observation of the characteristic wave visible above the background noise, and (2) by FFT analysis to screen for peaks at twice the stimulus frequency. This method is commonly used in fish AEP studies (Casper et al., 2003; Kenyon et al., 1998) and is based on the theory that the opposed orientation of the hair cells in the sacculus of the inner ear gives rise to the characteristic frequency response at twice the stimulus frequency (Fay, 1974). The visual estimate of the hearing threshold was defined as the lowest SPL that generated an AEP response in both the averaged trace and the FFT (Vetter et al., 2018).

Dead controls (10 in total) were frozen for a minimum of 24 h and defrosted prior to the control experiment. Control experiments were run according to the same protocol, including the positioning of the electrodes. No AEPs were elicited from any of these control specimens, confirming that the AEPs recorded in this study represent electrophysiological responses from live sharks and were not artefacts from the experimental setup.

Objective estimation of hearing thresholds

As suggested by Sisneros et al. (2016), we included an objective AEP threshold determination method, because visual methods

Table 2. Parameters of acoustic pip signals

Frequency (Hz)	Duration (ms)	Hanning window (ms)*	Presentation rate (s^{-1})	Recording window (ms)	Start SPL_{rms} (dB re. 1 µPa)	Start PAL_{rms} (dB re. 1 µm s^2)
80	50	3	8	100	142.3	97.4
100	50	3	8	100	140.7	94.6
150	50	3	8	100	151.7	104.4
200	50	3	8	100	150.7	100.5
300	50	3	8	100	149	103.5
450	25	3	8	100	149.6	113
600	25	3	8	100	149.9	114.2
800	25	3	8	100	150	113.4
1200	25	3	8	100	151.1	117.8

*Time applies for rise, fall and plateau, respectively.

Journal of Experimental Biology (2023) 226, jeb245973. doi:10.1242/jeb.245973

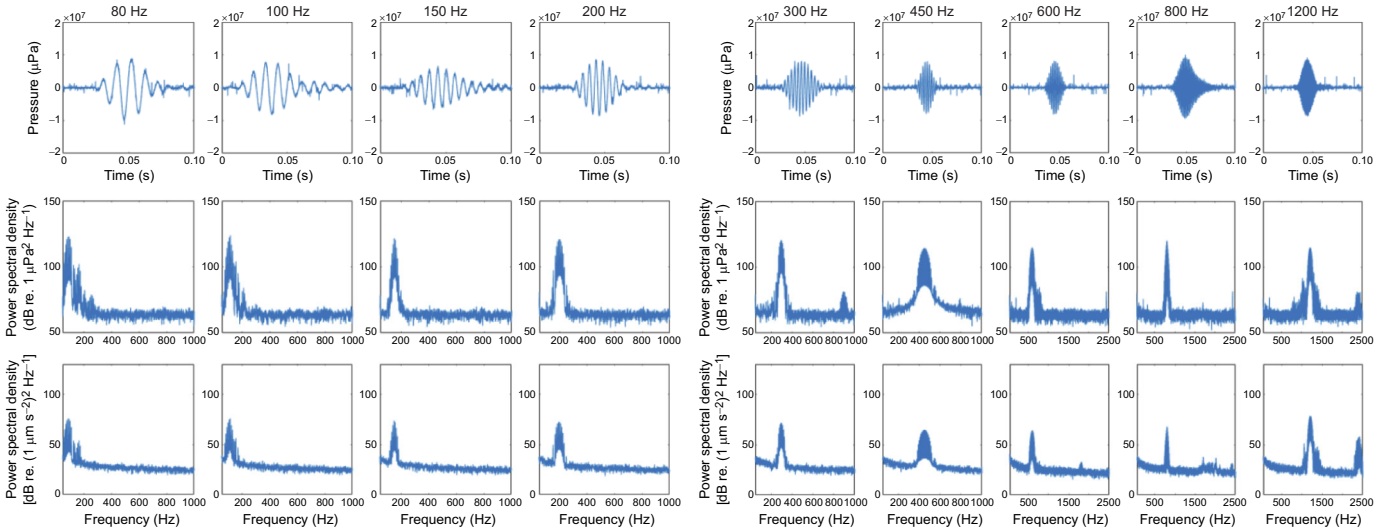

Fig. 2. Representative examples of the stimulus waveforms for test frequencies of 80–1200 Hz. The corresponding power spectra are plotted below each waveform for both pressure (dB re. 1 μPa^2 Hz^{-1}) and particle acceleration [dB re. (1 μm s^{-2})^2 Hz^{-1}]. All tone-bursts are shown at a sound pressure level of 135 dB re. 1 μPa. Measurements were made using a hydrophone and a triaxial accelerometer in the same place, where the shark's inner ear was positioned.

alone were shown to be subject to observer bias (Xiao and Braun, 2008). The '*x*-intercept' estimation method applied here has previously been used in hearing studies with marine mammals (Nachtigall et al., 2004, 2007), cephalopods (Mooney et al., 2010) and crustaceans (Dinh and Radford, 2021; Jézéquel et al., 2021). First, the 2048-point fast Fourier transform (FFT) power spectra was calculated for 5–12 averaged waveforms per frequency, using a custom-written MATLAB script (see Fig. 5 for example). As with fish AEPs, the spectra revealed peaks at twice the stimulus frequency at suprathreshold and a decrease in FFT peak amplitude corresponded with decreasing SPLs (Maruska and Sisneros, 2016). Second, the maximum FFT values (peak value) were found across five FFT bins greater than the presented frequencies and five FFT bins less than twice the presented frequencies and were plotted against the presented SPL (see Fig. 5D). Third, a series of regressions was run, that included 3, then 4, 5, to the *i*th peak value. The regression line that yielded the highest r^2-value (best fitting line) was selected to calculate the *x*-intercept. The *x*-intercept of the best fitting line served as estimate of the animal's probable hearing threshold (Nachtigall et al., 2007).

Pressure and particle acceleration calibrations

Acoustic stimuli were calibrated at the beginning of every experimental day using a miniature reference hydrophone (TC4013, sensitivity −211 dB re. 1 V μPa^{-1}, Teledyne Reson Ltd, Slangerup, Denmark) placed inside the empty animal holder and held in place by rubber bands at the same location where the animal's inner ear would be located during the experiment. A digital oscilloscope (Tektronix DPO2014 digital phosphor oscilloscope) was used to measure the sound pressure level (SPL) at each frequency, which was then attenuated through SigGen to output the desired decibel levels. Filtered ambient noise readings were taken to ensure that background sound levels were similar between test days.

Acoustic particle motion is likely to be the most relevant stimulus for hearing in sharks, we subsequently measured the particle acceleration levels, associated with each determined pressure threshold. A waterproofed triaxial accelerometer (DeltaTron®, Type 4524, National Instruments, Austin, TX, USA; sensitivities: x=9.770 mV ms^{-2}, y=9.977 mV ms^{-2}, z=10.02 mV ms^{-2}) was placed into the fish holder and held in place by rubber bands in the position of the shark's inner ear. The sensors were aligned such that 'x' would be the along-body axis (head to tail), 'y' the left-right axis and the 'z' was the vertical axis. Data from the accelerometer were amplified with a Brüel & Kjær signal conditioning amplifier (NEXUS Type 2690-OS4, Nærum, Denmark) and the peak-to-peak voltage (V_{pk-pk}) measured on an oscilloscope (Tektronix DPO 2014). The V_{pk-pk} was converted to V_{rms} and the acceleration was calculated for the x, y and z planes and followed by the particle acceleration magnitude (μms^{-2}, calculated as $\sqrt{x^2+y^2+z^2}$).

Acoustic impedance measurements

As suggested by Popper et al. (2019) and Popper and Fay (2011), we report the acoustic impedance of the testing environment for all stimulus frequencies and compare it to the acoustic impedance in water in a free field. The acoustic impedance is defined as the ratio between sound pressure (Pa) and particle velocity (ms^{-2}). In contrast to a free-field environment, the ratio between the pressure and particle motion is unpredictable for a confined tank environment (Rogers et al., 2016). This is because the pressure to particle motion ratio changes with distance from the sound source, the water surface, the tank walls and the dimensions and material of the tank itself. Because sharks are sensitive to particle motion, their hearing thresholds would also depend on the acoustic impedance of the test environment. Therefore, the acoustic impedance of the experimental tank was determined at the location of the shark's inner ear at three relevant sound pressure levels (120, 135 and 140 dB re. 1 μPa SPL$_{rms}$) for all frequencies examined. A hydrophone (TC4013, sensitivity −211 dB re. 1 V μPa^{-1}; Teledyne Reson Ltd, Slangerup, Denmark) and a waterproofed, neutrally buoyant, triaxial accelerometer (DeltaTron®, Type 4524, National Instruments, Austin, TX, USA; sensitivities: x=9.770 mV ms^{-2}, y=9.977 mV ms^{-2}, z=10.02 mV ms^{-2}) were placed inside the empty animal holder and held in place by rubber bands in the same location as the shark's inner ear. Data from the accelerometer were amplified by a Brüel & Kjær signal conditioning amplifier (NEXUS Type 2690-OS4, Nærum,

Journal of Experimental Biology (2023) 226, jeb245973. doi:10.1242/jeb.245973

Denmark) and data from the hydrophone were filtered (HP: 50 Hz; LP: 1 kHz) and amplified by a charge amplifier (VP2000, Teledyne Reson Ltd, Slangerup, Denmark). The $V_{pk–pk}$ for both the pressure wave and the particle acceleration wave of the *x*-axis (along-body axis, head to tail) were measured on an oscilloscope (Tektronix DPO2014). The *x*-axis was chosen because the acoustic power was higher along this axis than along the *y*-axis (left–right) and *z*-axis (vertical), due to the position of the speaker 55 cm in front of the shark. Particle acceleration was transformed into particle velocity using the formula $v=a/2\pi f$ (Nedelec et al., 2016). Then, the impedance for each frequency was calculated in MRayl, where 1 Rayl=1 Pa s m^{-1}. These values were then compared with the theoretical free-field impedance of seawater with a salinity of 35 ppt and 15°C and represented on a log scale (dB re. 1.5597 MRayl) (Vetter et al., 2019). The phase of the impedance was estimated by measuring the phase difference ($\Delta\phi$) between the particle acceleration and the sound pressure wave. Based on the assumption that in the acoustic nearfield the phase of the particle velocity waveform leads the phase of the particle acceleration waveform by 90 deg, the phase of the impedance was then calculated as $\Delta\phi_{p,v}=\Delta\phi_{p,a}+90$ deg (Vetter et al., 2019).

Statistical analysis

The distributions of the response variables (pressure and PAL based AEP thresholds) were normal; hence no transformation of the data was needed. However, with only one individual showing a threshold at 800 Hz, this observation was removed from the analysis, because no comparisons could be made for that frequency.

The test tank was supplied with ambient seawater, and the water temperature ranged from 14.7 to 22.5°C over the course of the experimental period, depending on the season. Difference in water temperature can affect the latency and amplitude of the AEP response in marine invertebrates (Jézéquel et al., 2021; Mooney et al., 2010) and has been shown to affect AEP thresholds in some fish (Wysocki et al., 2009b). Sex and total length of the animal may potentially affect hearing abilities and to increase over the course of ontogeny in some species of elasmobranchs (Corwin, 1981c, 1983; Parmentier et al., 2020; Sauer et al., 2022). To test for any effects of water temperature, total length, and sex on AEP thresholds, linear mixed effects analyses were firstly conducted. PAL-based thresholds were fitted against temperature, total length and sex as the main effects and random intercepts for each shark subject. Data for each species were analysed in separate models and checked for linear and quadratic curve relationships, respectively. There was no association between threshold and temperature (carpet shark, t_4=0.87, P=0.43; rig shark, t_3=1.35, P=0.27; school shark, t_{37}=1.99, P=0.053), threshold and total length (carpet shark, t_4=0.13, P=0.91; rig shark, t_2=0.59, P=0.62; school shark,

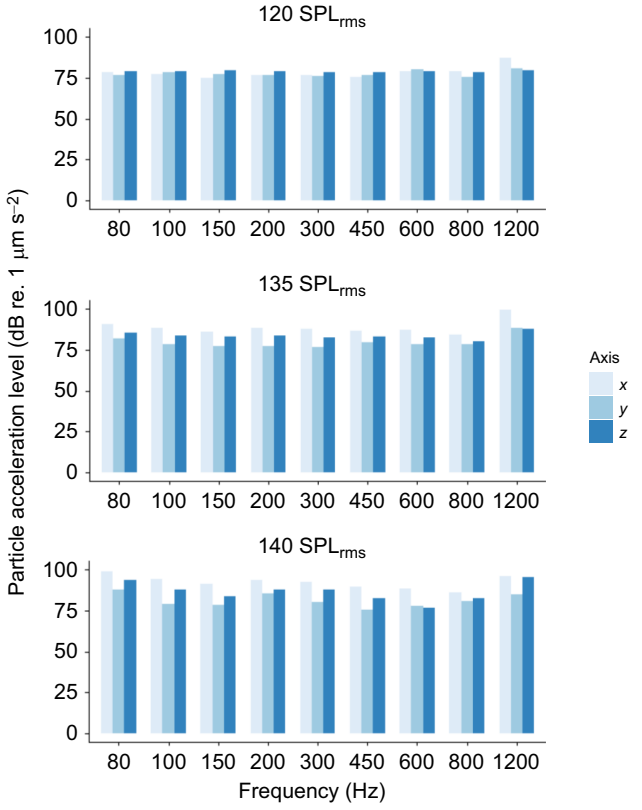

Fig. 3. Speaker-generated particle acceleration levels (dB re. 1 µm^{-2} PAL$_{rms}$) in all three dimensions. PAL at all frequencies examined for three sound pressure levels (SPL$_{rms}$): 120, 135 and 140 dB re. 1 µPa. Light blue, *x*-axis (anterior–posterior); medium blue, *y*-axis (medial–lateral); dark blue, *z*-axis (vertical). Measurements were made using a triaxial accelerometer where the shark's inner ear was positioned.

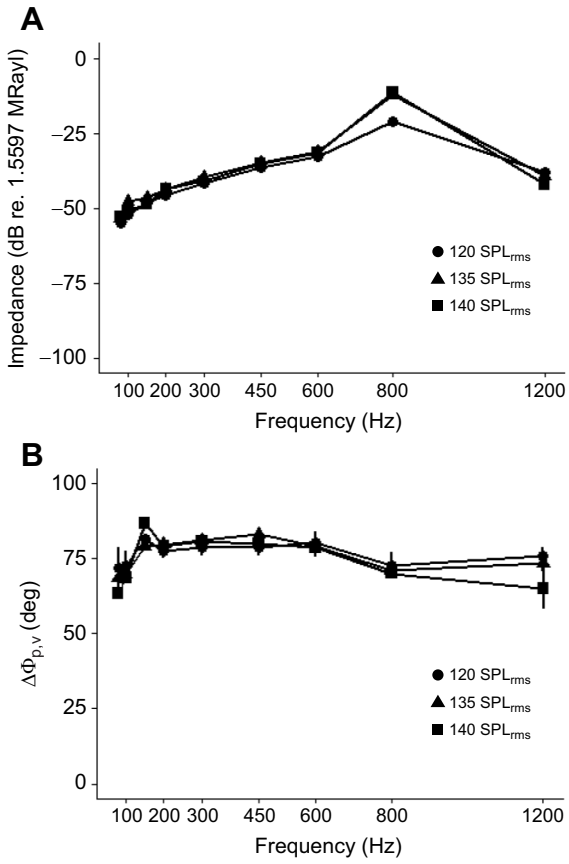

Fig. 4. Acoustic characteristics of the experimental tank and speaker. (A) Acoustic impedance [*Z*=ratio of sound pressure (Pa) to particle velocity (m s^{-1}) in *x*-direction] relative to 1.5597 MRayl (the reference impedance for a free-field in 35 ppt salinity seawater at 15°C, where 1 Rayl=1 Pa s m^{-1}) plotted for all the frequencies examined at three sound pressure levels (SPL$_{rms}$) 120, 135 and 140 dB re. 1 µPa. (B) Phase differences (Δ) between the pressure and particle velocity waves. Measurements (n=3 for each frequency and SPL) were made using a hydrophone and a triaxial accelerometer placed in the same place, where the shark's inner ear was positioned. All data are plotted as means±s.d.

Journal of Experimental Biology (2023) 226, jeb245973. doi:10.1242/jeb.245973

t_{37}=0.92, P=0.36), and threshold and sex (carpet shark, t_4=0.1, P=0.92; rig shark, t_2=−0.05, P=0.97; school shark, t_{37}=0.003, P=0.99) (Fig. S1). Therefore, all data could be grouped to increase sample size and power of the analysis.

To compare the two threshold determination methods (visual and statistical) within each species and each frequency a linear mixed-effects analysis was performed (Bates et al., 2015). Pressure and PAL based thresholds were fitted respectively against a factor, termed 'group' as the main effect and random intercepts for each shark subject. The group factor represents all possible combinations of the variables species, frequency, and method (e.g. Carpet.Shark_80Hz_visual, Carpet.Shark_80Hz_statistical, Rig.Shark_80Hz_visual, etc.). This factor was needed for the models to run properly, as there was not enough overlap in the distribution of frequencies, because the carpet shark did not show any responses at 450, 600 Hz. *Post hoc* pairwise comparisons were used to explore differences between threshold means between methods (within each species and each frequency). Only comparisons within the same species and frequency were examined (e.g. Carpet.Shark_80Hz_visual vs. Carpet.Shark_80Hz_statistical). All between species and 'nonsensical' comparisons (e.g. Carpet.Shark_80Hz_visual vs. Rig.Shark_100Hz_statistical) were ignored.

To compare statistically derived thresholds between species within each frequency, linear mixed-effects analyses were performed taking only the data from the statistical method into account. Pressure- and PAL-based thresholds were fitted against a factor, termed 'group' (representing all possible combinations of the variables species, frequency, e.g. Carpet.Shark_80 Hz, Rig.Shark_80 Hz, School.Shark_80 Hz, etc.) as the main effect and random intercepts for each shark subject. *Post hoc* pairwise comparisons were used to explore differences between threshold means between species (within frequencies). Only comparisons between species (within frequency) were examined (e.g. Carpet.Shark_80 Hz vs. Rig.Shark_80 Hz). All 'nonsensical' or within-species comparisons (e.g. Carpet.Shark_80 Hz vs. Carpet.Shark_100 Hz) were ignored.

P-values were adjusted using the FDR method and all statistical tests were considered significant at P<0.05. All statistical analyses

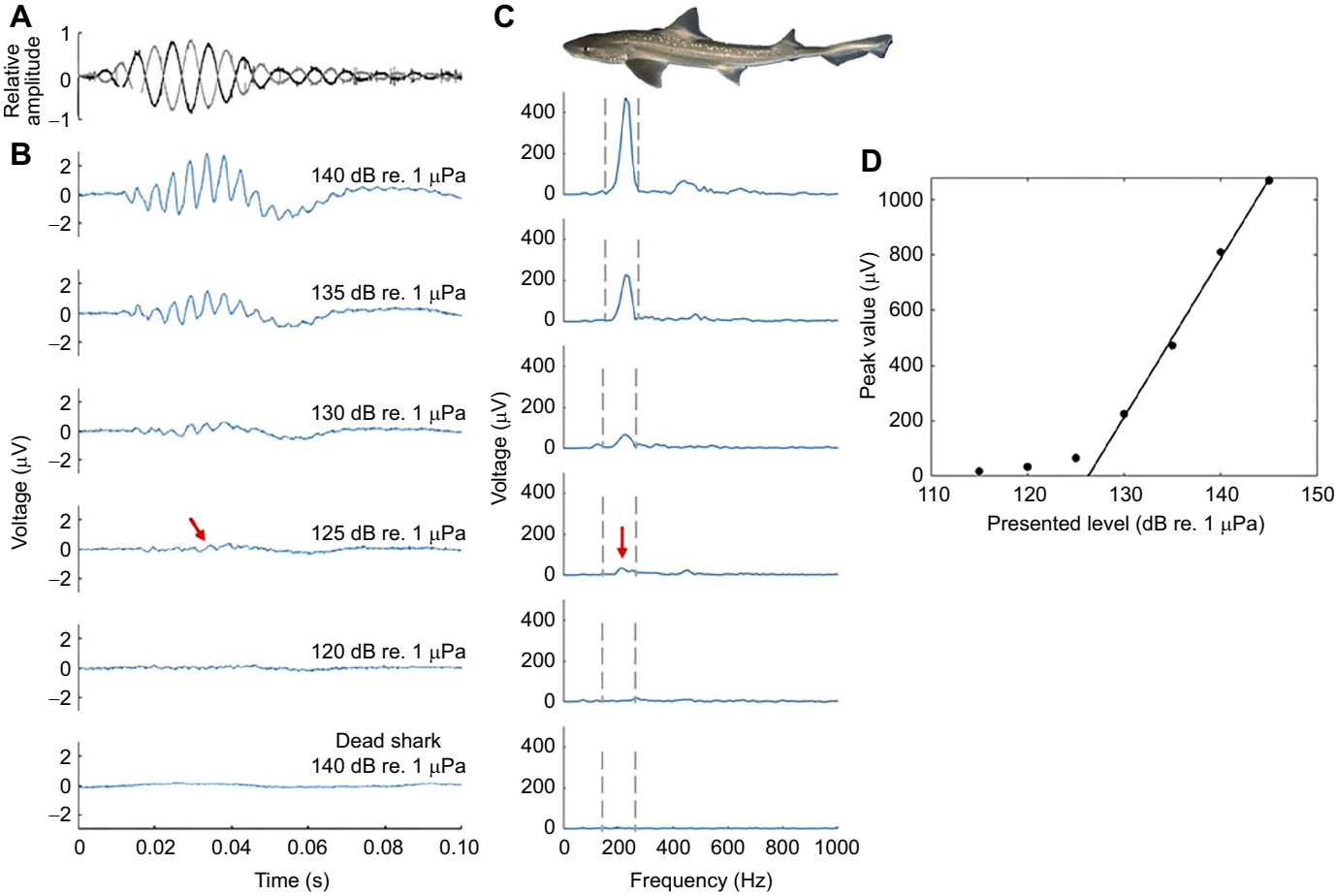

Fig. 5. Characteristic examples of speaker-generated AEP waveforms with corresponding FFT spectra and threshold determination procedures shown for a rig shark (*Mustelus lenticulatus*). (A) Examples shown for a 100 Hz Hann-gated acceleration signal (50 ms) presented at opposing polarities of 0 deg (black) and 180 deg (grey). (B) Average AEP waveforms were collected for signal levels ranging from 145 to 120 dB re. 1 µPa SPL_{rms} in decreasing steps of 5 dB. Each response was collected using 1200 sweep averages (600 at a stimulus polarity of 0 deg and 600 at 180 deg). The red arrow highlights the lowest visually distinguishable responses at 125 dB re. 1 µPa SPL_{rms}. The last trace shows the control test where the active electrode was in the standard recording position, but the animal was dead. (C) Corresponding 2048 point FFTs of the entire 100 ms duration of the traces. The peak frequency of the observed responses was twice the frequency of the 100 Hz tone-pip stimulus (200 Hz shown by the red arrow). The maximum FFT value was found across the five FFT bins greater than and five FFT bins less than twice the presented frequency (143–262 Hz) as delineated by the dotted grey lines. (D) For statistical threshold determination, the maximum FFT voltage (peak value) between these frequency bins was plotted against the presented sound pressure level, and the *x*-intercept of the best fitting regression line was used as estimate of the animal's AEP threshold. The statistically derived AEP threshold at 100 Hz for this individual was 126.26 dB re. 1 µPa SPL_{rms}.

Journal of Experimental Biology (2023) 226, jeb245973. doi:10.1242/jeb.245973

were performed in R (v.4.1.1; https://www.r-project.org/) using lmer in lme4 (https://CRAN.R-project.org/package=lme4) and emmeans (v.1.6; https://CRAN.R-project.org/package=emmeans) packages.

RESULTS

Acoustic characteristics of the experimental tank

Fast Fourier transformation analyses of the presented stimuli waveforms reveal clear spectral peaks at the respective stimulus frequencies (Fig. 2). No acoustic energy was contained in any higher-order harmonics, except for 1200 Hz, which was well outside the hearing range of these three animals.

For lower signal levels (e.g. 120 dB re. 1 µPa), the acoustic energy was equally distributed among the three axes, whereas for higher signal levels (e.g. 135 dB re. µPa) the along-body axis (*x*: 88.5±4.4 dB re. 1 µms^{-2}) had the highest accelerations compared with the *y*-axis (79.3±3.6 dB re. 1 µms^{-2}) and *z*-axis (83.4±2 dB re. 1 µms^{-2}) across all test frequencies (Fig. 3). As expected, the impedance values of our test tank were much lower than in a free-field environment (Fig. 4A). This means that the particle acceleration levels, associated with any given sound pressure level, were much higher than what would be expected in the acoustic far field in an unbound medium. Furthermore, these results also indicate that there were no major resonances in the tank at any of the test frequencies (Fig. 4B).

AEP waveform characteristics

The AEP waveforms of the three shark species were similar in shape and time course and showed a sharp peak at twice the stimulus frequency in the FFT analysis at suprathreshold levels (Fig. 5). A typical suprathreshold AEP response consisted of a series of downward and upward peaks superimposed over a slow negative deflection, that was generally followed by a slow positive deflection, as it is typically described for other fishes (Bullock and Corwin, 1979; Corwin et al., 1982; Kenyon et al., 1998).

Comparison between visually and statistically derived AEP thresholds

The shape and slope of visually and statistically determined threshold curves were similar; however, the statistically derived thresholds were consistently below the visually derived thresholds. For both the pressure and PAL determined thresholds, the statistical estimates were on average ∼4 dB re. 1 µPa below the visual estimates (Fig. 6, Tables S1,S2).

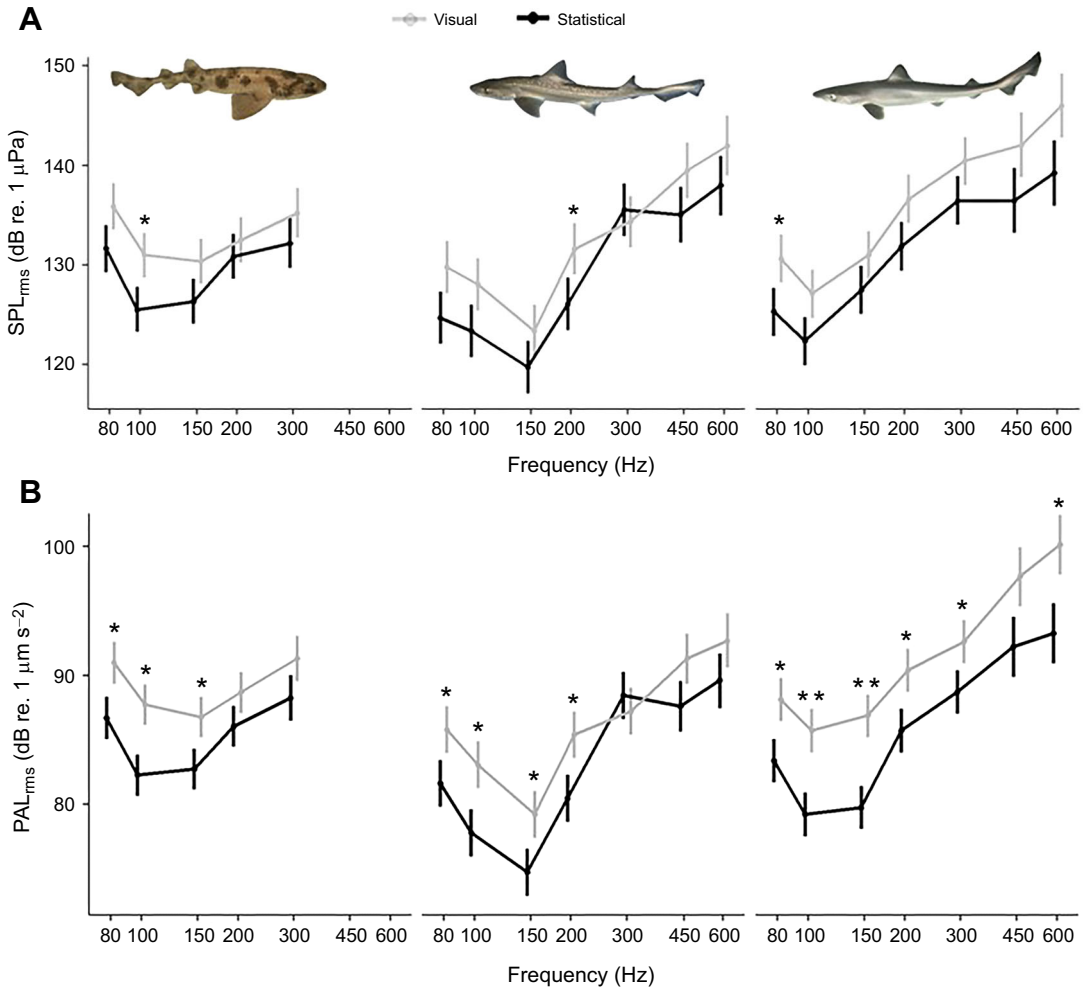

Fig. 6. Comparison of visual and statistical (objective) threshold determination methods. Visually (grey) and statistically (black) derived AEP threshold curves are shown for (left to right) the carpet shark (*Cephaloscyllium isabellum*), rig shark (*Mustelus lenticulatus*) and school shark (*Galeorhinus galeus*). Thresholds are shown based on (A) sound pressure level (dB re. 1 µPa SPL$_{rms}$) and (B) particle acceleration level (dB re. 1 µm s^{-2} PAL$_{rms}$). All data shown as mean (±1 s.e.m.). Means that are significantly different by Tukey test *post hoc* pairwise comparisons within each species and frequency: ***P*<0.001; **P*<0.05. Carpet shark, *N*=8; rig shark, *N*=6; school shark, *N*=7.

Journal of Experimental Biology (2023) 226, jeb245973. doi:10.1242/jeb.245973

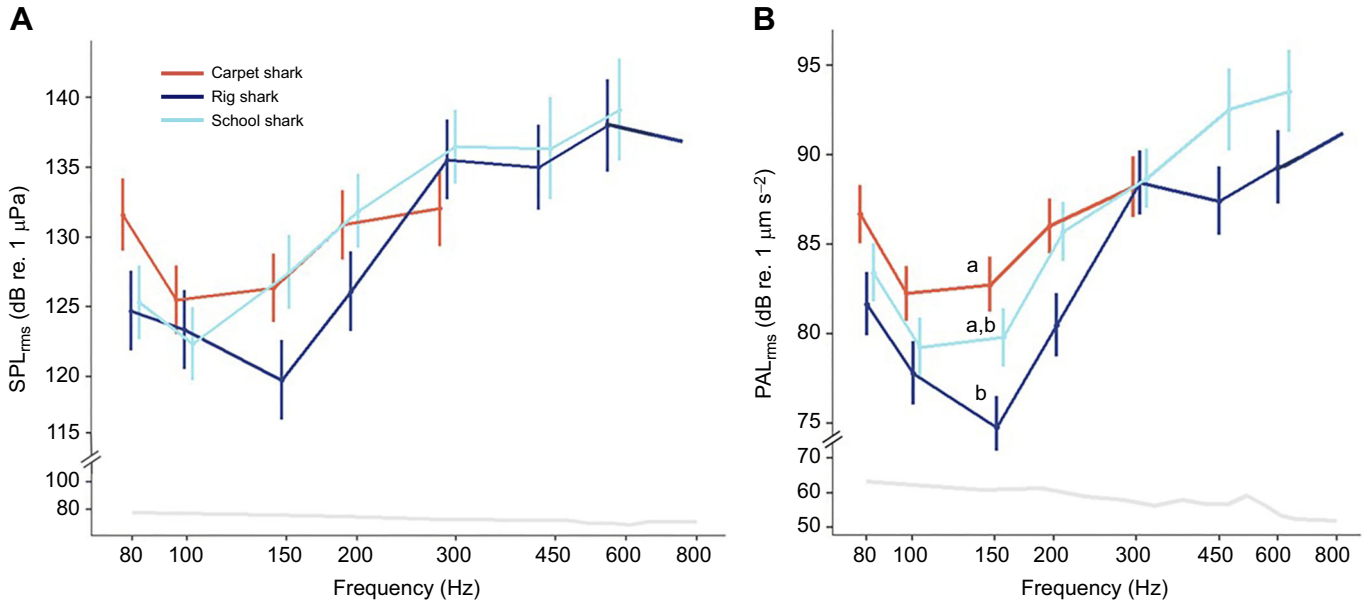

Fig. 7. AEP sensitivities for the carpet shark, rig shark and school shark measured in a tank and underwater speaker setup. Thresholds were determined statistically using the *x*-intercept method and are shown as mean (±1 s.e.m.) in terms of (A) sound pressure level (dB re. 1 µPa SPL_{rms}) and (B) particle acceleration level (dB re. 1 µm s^{-2} PAL_{rms}). Grey lines indicate ambient sound levels. Lowercase letters indicate results of *post hoc* pairwise comparisons between species, within each frequency. Means not sharing any common letter are significantly different by the Tukey test at the 5% level of significance. To improve readability, letters were omitted when no significant difference was detected between means. Carpet shark, *N*=8; rig shark, *N*=6; school shark, *N*=7.

Comparison of statistically derived AEP thresholds between different species

Detection threshold curves for pressure and PAL are similar in shape and slope within each species, with sensitivity maxima and minima at the same frequencies (Fig. 7). Pressure thresholds were similar between the three species (Fig. 7A; Table S3). However, PAL thresholds showed that at 150 Hz the rig shark was more sensitive (P=0.004; 74.8±1.8 dB re. 1 µms^{-2} PAL_{rms}) than the carpet shark (82.8±2.5 dB re. 1 µms^{-2} PAL_{rms}), but not the school shark (79.8±1.6 dB re. 1 µms^{-2} PAL_{rms}) (Fig. 7B; Table S4). All sharks except one responded at frequencies from 80 to 300 Hz, while less than half responded at higher frequencies, and only one rig and none of the school sharks responded at 800 Hz (Fig. 8).

The carpet shark showed the narrowest hearing bandwidth (80–300 Hz), with the lowest mean threshold observed at 100 Hz (SPL_{rms}: 125.5±2.5 dB re. 1 µPa; PAL_{rms}: 82.3±1.5 dB re. 1 µms^{-2}). The rig shark showed the broadest hearing bandwidth (80–800 Hz) and was most sensitive to sounds below 300 Hz, with the lowest mean threshold observed at 150 Hz (119.8±2.5 dB re. 1 µPa SPL_{rms}/ 74.8±1.8 dB re. 1 µms^{-2} PAL_{rms}). Finally, the school shark responded from 80 to 600 Hz and was most sensitive to frequencies below 200 Hz, with lowest mean thresholds observed at 100 Hz (122.4±2.6 dB re. 1 µPa SPL_{rms}/ 79.3±1.6 dB re. 1 µms^{-2}, PAL_{rms}).

The background SPL_{rms} and PAL_{rms} in the tank (47–1200 Hz) ranged from 81 to 69 dB re. 1 µPa SPL_{rms} and from 65.3 to 52 dB re. 1 µms^{-2}, respectively, and was below the shark detection thresholds determined here.

DISCUSSION

This study provides novel baseline auditory sensitivity data for three ecologically distinct species of sharks, a fish group of which hearing abilities are largely unknown. Auditory evoked potential detection thresholds were quantified in response to pure tone acoustic stimuli from an underwater speaker. It was found that the three sharks were similar in their overall sensitivities but differed with respect to their upper frequency limits. The bottom dwelling carpet shark had the narrowest frequency detection range (80–300 Hz). Bandwidths were broader for the benthopelagic rig shark (80–800 Hz) and school shark (80–600 Hz). These results show that although hearing abilities were restricted to low frequencies, they do vary between species, suggesting that sound likely plays different roles in these species. Further studies comparing the anatomical structures of the inner ears in the three species are needed to determine which morphological adaptations may be responsible for the observed difference in detectable frequency range.

It is difficult to compare AEP thresholds with behaviourally derived thresholds (Hawkins, 1981). The AEP technique requires the fish to be restrained, often by use of anaesthesia, thus providing information on the response properties of the auditory system at the level of the brainstem, but not at the level of the whole animal (Sisneros et al., 2016). AEP thresholds in fish were shown to be above (~10 dB) behavioural thresholds at frequencies below 1 kHz (Ladich and Fay, 2013; Popper et al., 2019). In addition, absolute hearing thresholds vary greatly between different studies, because of differences in experimental setups and acoustic environments, making quantitative comparisons of threshold levels impossible (Ladich and Wysocki, 2009; Ladich and Fay, 2013). However, AEP threshold curves and behavioural audiograms can be used to estimate the auditory bandwidth of a species (Ladich and Fay, 2013; Vetter et al., 2018).

It is important to note that we were not able to test frequencies below 80 Hz, owing to tank acoustics, and speaker limitations. Therefore, it is very likely that the species examined here can detect frequencies well below 80 Hz, as has been shown for other species of sharks. For instance, the horn shark (*Heterodontus francisi*) (Casper and Mann, 2007a), bamboo sharks (*Chiloscyllium plagiosum* and *Chiloscyllium punctatum*) (Casper and Mann, 2007a,b) and the Atlantic sharpnose shark (*Rhizoprionodon*

Journal of Experimental Biology (2023) 226, jeb245973. doi:10.1242/jeb.245973

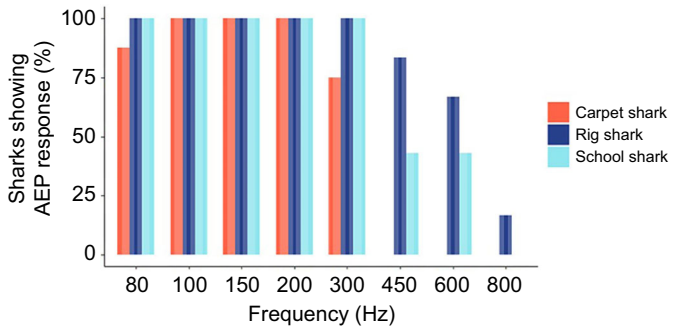

Fig. 8. Percentage of sharks that showed AEP responses to acoustic stimuli from an underwater speaker at each test frequency. Note that almost all sharks (20 of 21) across the three species responded from 80 Hz to 200 Hz, whereas fewer individuals responded to frequencies above 200 Hz AEPs, even at the highest sound pressure levels evaluated. Carpet shark, *N*=8; rig shark, *N*=6; school shark, *N*=7.

terranovae) (Casper and Mann, 2009) showed AEP responses to frequencies as low as 20 Hz. And the lemon shark (*Negaprion brevirostris*) has been shown to respond to frequencies as low as 10 Hz in behavioural experiments (Nelson, 1967).

The habitat and lifestyle of a species (e.g. motionless on the seafloor versus swimming in midwater) was proposed as a potential determining factor of the upper hearing limit in elasmobranchs (Corwin, 1981a; Mickle and Higgs, 2022). The present study showed that the demersal carpet shark has a low upper frequency limit of 300 Hz, compared with the more active, benthopelagic school and rig sharks that respond at 600 and 800 Hz, respectively. Physiological and behavioural evidence in other benthic sharks, such as *C. pliagiosum*, *H. francisi* (Casper and Mann, 2007a; Kelly and Nelson, 1975) and the cloudy catshark (*Scyliorhinus torazame*) (Ahn et al., 2011) suggest equally low upper frequency limits (max 300 Hz). However, Corwin's habitat-niche hypothesis to predict hearing abilities in elasmobranchs (Corwin, 1977, 1981a,b,c, 1989) does not apply to all bottom-dwelling species, as some strictly benthic species have been shown to detect frequencies of up to 1 kHz. For instance, AEP measurements in the bottom-dwelling, small spotted catshark (*Scyliorhinus canicula*) showed an upper frequency limit at 600 Hz (Parmentier et al., 2020) and nurse shark (*Ginglymostoma cirratum*) 1000 Hz (Casper and Mann, 2006). Similarly, benthic batoid species have all showed upper frequency limits of ∼800–1000 Hz (Casper et al., 2003; Casper and Mann, 2006; Corwin, 1983; Mickle et al., 2020). Habitat and feeding strategies likely contribute to hearing abilities in elasmobranchs, but there may be other factors (e.g. predation risk, reproduction strategies) driving interspecies differences in elasmobranch hearing abilities. There is currently a lack of audiometric data for any of the more basal Squalomorphii sharks, deep-sea or purely oceanic species as these are very difficult to keep in captivity (Corwin, 1989). Further comparative physiological, behavioural and anatomical studies in more species representative of different lifestyles and habitats are needed to resolve the ecological drivers for differences in hearing abilities in elasmobranchs.

The bandwidths and peak sensitivities of AEP detection thresholds of the sharks tested here are comparable with teleost species that only detect particle motion (Ladich and Fay, 2013; Popper and Fay, 2011). Examples are the flatfishes, such as common dab (*Limanda limanda*) and European plaice (*Pleuronectes platessa*), that have narrow hearing ranges (30–250 Hz) with best hearing at or below 110–160 Hz (Chapman and Sand, 1974); the common triple fin (*Forsterygion lapillum*) with peak sensitivity of 100–200 Hz (Radford et al., 2012); the red-mouthed goby (*Gobius cruentatus*) with upper limit at 700 Hz and peak sensitivity at 100–200 Hz (Wysocki et al., 2009a) and kawakawa (*Euthynnus affinis*) with upper limit at 800 Hz and peak sensitivity at 500–600 Hz (Iversen, 1969). The low frequency bandwidth observed in the sharks support previous experimental evidence suggesting that sharks only detect particle motion (Banner, 1967; Kelly and Nelson, 1975).

The results of this study must be evaluated with respect to the limitations of the acoustical setup and the measurement approach. Tank acoustics are very complicated, due to complex interactions of the sound with the water–air boundary and the tank walls (Parvulescu, 1964; Rogers et al., 2016). Therefore, the acoustic condition in the test tank experienced by the shark is very different from the natural free-field environment (Gray et al., 2016; Larsen and Radford, 2018; Popper and Hawkins, 2021). A small sound pressure generated within the tank will produce much larger particle motion than would be the case in the natural environment (Parvulescu, 1964). As a result, the hearing abilities of the sharks may be unnaturally extended to higher frequencies in a tank setting (Chapman and Sand, 1974). Ideally, hearing thresholds should be measured in the free field (e.g. Chapman and Sand, 1974; Hawkins and Chapman 1975; Hawkins and Johnstone, 1978). It would be particularly interesting to conduct free field experiments within both the acoustic near field and far field, to solve the currently unanswered question of how far from a sound source sharks can detect sound (Casper and Mann, 2006, 2009). In this study, the shark was positioned within the acoustic nearfield [assuming the boundary of the acoustic nearfield for a monopole source is approximately equal to $\lambda/2\pi$ (Yan, Anraku, & Babaran, 2010)], which the impedance results confirm (Vetter et al., 2019). In addition, in the nearfield, there exists hydrodynamic flow that is generated by the vibrations of the underwater loudspeaker (Kalmijn, 1988). In some teleost fishes, the lateral line responds to these flows at frequencies up to 200 Hz. (Braun and Coombs, 2000; Harris and van Bergeijk, 1962; Higgs and Radford, 2013; Hueter et al., 2004; Maruska and Sisneros, 2016). Therefore, the AEP responses measured at frequencies below 200 Hz may potentially contain contributions from the lateral line system.

Conclusions

In summary, this study assessed AEP sensitivities to acoustic stimuli from an underwater speaker in the benthic New Zealand carpet shark, the benthopelagic rig and the school shark. The three species have similar sensitivities but differ in their upper frequency limit. Our results indicate that the hearing abilities of the three shark species were most consistent with those known for hearing 'non-specialists' fishes that detect only the particle motion component of the sound field. Furthermore, our results provide evidence that benthopelagic sharks can hear higher frequencies (max. 800 Hz) than some of the bottom dwelling sharks (max. 300 Hz). Finally, the AEP detection thresholds presented here provide a good first approximation of the basic hearing abilities for the three shark species. However, further behavioural and morphological studies are needed to test which ecological factors are driving the observed interspecific differences in hearing bandwidth.

Acknowledgements

The authors would like to thank Errol Murray, Gavin Perry, Derek Sauer, Stefan Spreitzenbarth, and Stefano Schoene from the Leigh Marine Lab for their help with the animal collections. We would like to express our gratitude to Jenni Stanley and Paul Caiger for their help troubleshooting the AEP setup. We are grateful to Jessica McLay and Jason P. Dinh for help with statistics.

Competing interests
The authors declare no competing or financial interests.

Author contributions
Conceptualization: C.N., J.C.M., C.A.R.; Methodology: C.N., J.R., C.A.R.; Software: J.R.; Validation: C.N.; Formal analysis: C.N.; Investigation: C.N.; Resources: J.C.M., C.A.R.; Data curation: C.N.; Writing - original draft: C.N.; Writing - review & editing: J.C.M., C.A.R.; Visualization: C.N.; Supervision: J.R., J.C.M., C.A.R.; Project administration: C.A.R.; Funding acquisition: C.N., J.C.M., C.A.R.

Funding
This project was funded by a Marsden grant (UOA1808 to C.A.R.) and by a University of Auckland Doctoral Scholarship to C.N.

Data availability
All relevant data can be found within the article and its supplementary information.

ECR Spotlight
This article has an associated ECR Spotlight interview with Carolin Nieder.

References

Ahn, J. Y., Choi, C. M. and Lee, C. H. (2011). Auditory characteristics of tiger shark (*Scyliorhinus torazame*) caught in the coast of Jeju Island. *J. Kor. Soc. Fish. Ocean Tech.* **47**, 234-240. doi:10.3796/KSFT.2011.47.3.234
Backus, R. H. (1963). Hearing in elasmobranchs. In *Sharks and survival* (ed. G. W. Perry), pp. 243-254. Boston, MA, USA: D. C. Heath and Company.
Banner, A. (1967). Evidence of sensitivity to acoustic displacements in the lemon shark, *Negaprion brevirostris* (Poey). In *Lateral Line Detectors* and (ed. P. , Cahn), pp. 265-273. New York, NY, USA: Indiana University Press.
Banner, A. (1972). Use of sound in predation by young lemon sharks, *Negaprion brevirostris* (Poey). *Bull. Mar. Sci.* **22**, 251-283.
Bates, D., Mächler, M., Bolker, B. and Walker, S. (2015). Fitting linear mixed-effects models using lme4. *J. Stat. Softw.* **67**, 1-48. doi:10.18637/jss.v067.i01
Braun, C. B. and Coombs, S. (2000). The overlapping roles of the inner ear and lateral line: the active space of dipole source detection. *Philos. Trans. R. Soc. Lond. B: Biol. Sci.* **355**, 1115-1119. doi:10.1098/rstb.2000.0650
Bullock, T. H. and Corwin, J. T. (1979). Acoustic evoked activity in the brain in sharks. *J. Comp. Physiol. A* **129**, 223-234. doi:10.1007/BF00657658
Carrier, J. C., Pratt, H. L. and Martin, L. K. (1994). Group reproductive behaviors in free-living nurse sharks, *Ginglymostoma cirratum*. *Copeia* **1994**, 646-656. doi:10.2307/1447180
Casper, B. M. and Mann, D. A. (2006). Evoked potential audiograms of the nurse shark (*Ginglymostoma cirratum*) and the yellow stingray (*Urobatis jamaicensis*). *Environ. Biol. Fishes* **76**, 101-108. doi:10.1007/s10641-006-9012-9
Casper, B. M. and Mann, D. A. (2007a). Dipole hearing measurements in elasmobranch fishes. *J. Exp. Biol.* **210**, 75-81. doi:10.1242/jeb.02617
Casper, B. M. and Mann, D. A. (2007b). The directional hearing abilities of two species of bamboo sharks. *J. Exp. Biol.* **210**, 505-511. doi:10.1242/jeb.02677
Casper, B. M. and Mann, D. A. (2009). Field hearing measurements of the Atlantic sharpnose shark *Rhizoprionodon terraenovae*. *J. Fish Biol.* **75**, 2768-2776. doi:10.1111/j.1095-8649.2009.02477.x
Casper, B. M., Lobel, P. S. and Yan, H. Y. (2003). The hearing sensitivity of the little skate, *Raja erinacea*: a comparison of two methods. *Environ. Biol. Fishes* **68**, 371-379. doi:10.1023/B:EBFI.0000005750.93268.e4
Chapman, C. and Sand, O. (1974). Field studies of hearing in two species of flatfish *Pleuronectes platessa* (L.) and *Limanda limanda* (L.) (Family Pleuronectidae). *Comp. Biochem. Physiol. A: Physiol.* **47**, 371-385. doi:10.1016/0300-9629(74)90082-6
Chapuis, L. and Collin, S. P. (2022). The auditory system of cartilaginous fishes. *Rev. Fish Biol. Fish.* **32**, 521-554. doi:10.1007/s11160-022-09698-8
Chapuis, L., Collin, S. P., Yopak, K. E., Mccauley, R. D., Kempster, R. M., Ryan, L. A., Egeberg, C. A., Kerr, C. C., Gennari, E., Egeberg, C. A. et al. (2019). The effect of underwater sounds on shark behaviour. *Sci. Rep.* **9**, 6924. doi:10.1038/s41598-019-43078-w
Christensen, C. B., Christensen-Dalsgaard, J., Madsen, P. T. (2015). Hearing of the African lungfish (*Protopterus annectens*) suggests underwater pressure detection and rudimentary aerial hearing in early tetrapods. *J. Exp. Biol.* **218**, 381-387. doi:10.1242/jeb.116012
Corwin, J. T. (1977). Morphology of the macula neglecta in sharks of the genus *Carcharhinus*. *J. Morphol.* **152**, 341-361. doi:10.1002/jmor.1051520306
Corwin, J. T. (1978). The relation of inner ear structure to the feeding behavior in sharks and rays. In *Scanning Electron Microscopy* (ed. O. Johari), pp. 1105-1112. S.E.M. Inc.
Corwin, J. T. (1981a). Audition in elasmobranchs. In *Hearing and Sound Communication in Fishes* (ed. W. N. Tavolga, A. N. Popper and R. R. Fay), pp. 81-105. Springer. doi:10.1007/978-1-4615-7186-5_5
Corwin, J. T. (1981b). Peripheral auditory physiology in the lemon shark: evidence of parallel otolithic and non-otolithic sound detection. *J. Comp. Physiol.* **142**, 379-390. doi:10.1007/BF00605450
Corwin, J. T. (1981c). Postembryonic production and aging of inner ear hair cells in sharks. *J. Comp. Neurol.* **201**, 541-553. doi:10.1002/cne.902010406
Corwin, J. T. (1983). Postembryonic growth of the macula neglecta auditory detector in the ray, *Raja clavata*: continual increases in hair cell number, neural convergence, and physiological sensitivity. *J. Comp. Neurol.* **217**, 345-356. doi:10.1002/cne.902170309
Corwin, J. T. (1989). Functional anatomy of the auditory system in sharks and rays. *J. Exp. Zool.* **252**, 62-74. doi:10.1002/jez.1402520408
Corwin, J. T., Bullock, T. H. and Schweitzer, J. (1982). The auditory brain stem response in five vertebrate classes. *Electroencephalogr. Clin. Neurophysiol.* **54**, 629-641. doi:10.1016/0013-4694(82)90117-1
Dinh, J. P. and Radford, C. A. (2021). Acoustic particle motion detection in the snapping shrimp (*Alpheus richardsoni*). *J. Comp. Physiol. A* **207**, 641-655. doi:10.1007/s00359-021-01503-4
Ebert, D. A., Dando, M. and Fowler, S. (2021). *A pocket guide to sharks of the world*. Princeton University Press. doi:10.2307/j.ctv1cmsmwn
Fay, R. R. (1974). Sound reception and processing in the carp: saccular potentials. *Comp. Biochem. Physiol. A: Physiol.* **49**, 29-42. doi:10.1016/0300-9629(74)90539-8
Fay, R. R. and Popper, A. N. (2000). Evolution of hearing in vertebrates: the inner ears and processing. *Hear. Res.* **149**, 1-10. doi:10.1016/S0378-5955(00)00168-4
Fay, R. R., Kendall, J. I., Popper, A. N. and Tester, A. L. (1974). Vibration detection by the macula neglecta of sharks. *Comp. Biochem. Physiol. A: Physiol.* **47**, 1235-1240. doi:10.1016/0300-9629(74)90097-8
Fetterplace, L. C., Esteban, J. D., Pini–Fitzsimmons, J., Gaskell, J. and Wueringer, B. E. (2022). Evidence of sound production in wild stingrays. *Ecol. Soc. Am.* **103**, e3812. doi:10.1002/ecy.3812
Flock, A. (1971). Sensory transduction in hair cells. In *Principles of Receptor Physiology* (ed. W. Loewenstein), pp. 396-441. Springer. doi:10.1007/978-3-642-65063-5_14
Flock, A. and Wersall, J. (1963). Morphological polarization and orientation of hair cells in labyrinth and lateral line organ. *J. Ultrast. Res.* **8**, 193-194.
Francis, M. P. and Francis, R. (1992). Growth rate estimates for New Zealand rig (*Mustelus lenticulatus*). *Mar. Freshw. Res.* **43**, 1157-1176. doi:10.1071/MF9921157
Francis, M. P. and Mulligan, K. P. (1998). Age and growth of New Zealand school shark, *Galeorhinus galeus*. *N. Z. J. Mar. Freshw. Res.* **32**, 427-440. doi:10.1080/00288330.1998.9516835
Francis, M. P., Lyon, W., Jones, E., Notman, P., Parkinson, D. and Getzlaff, C. (2012). Rig nursery grounds in New Zealand: a review and survey. New Zealand Aquatic Environment and Biodiversity Report. (No. 95). https://fs.fish.govt.nz/Page.aspx?pk=113&dk=23023
Gray, M. D., Rogers, P. H., Popper, A. N., Hawkins, A. D. and Fay, R. R. (2016). "Large" tank acoustics: how big is big enough? In *The Effects of Noise on Aquatic Life II* (ed. A. N. Popper and A. D. Hawkins), pp. 363-369. Springer. doi:10.1007/978-1-4939-2981-8_43
Harris, G. G. and Van Bergeijk, W. A. (1962). Evidence that the lateral–line organ responds to near-field displacements of sound sources in water. *J. Acoust. Soc. Am.* **34**, 1831-1841. doi:10.1121/1.1909138
Hawkins, A. D. (1981). The hearing abilities of fish. In *Hearing and Sound Communication in Fishes* (ed. W. N. Tavolga, A. N. Popper and R. R. Fay), pp. 109-137. Springer. doi:10.1007/978-1-4615-7186-5_6
Hawkins, A. D. and Chapman, C. (1975). Masked auditory thresholds in the cod, *Gadus morhua* L. *J. Comp. Physiol.* **103**, 209–226. doi:10.1007/BF00617122
Hawkins, A. D. and Johnstone, A. (1978). The hearing of the Atlantic Salmon, *Salmo salar*. *J. Fish Biol.* **13**, 655-673. doi:10.1111/j.1095-8649.1978.tb03480.x
Higgs, D. M. and Radford, C. A. (2013). The contribution of the lateral line to 'hearing' in fish. *J. Exp. Biol.* **216**, 1484-1490. doi:10.1242/jeb.078816
Horn, P. L. (2016). Biology of the New Zealand carpet shark *Cephaloscyllium isabellum* (Scyliorhinidae). *J. Ichthyol.* **56**, 336-347. doi:10.1134/S0032945216030048
Hueter, R. E., Mann, D. A., Maruska, K. P., Sisneros, J. A. and Demski, L. S. (2004). Sensory biology of elasmobranchs. In *Biology of Sharks and Their Relatives* (ed. P. L. Lutz), pp. 325-368. CRC Press; Taylor & Francis Group.
Iversen, R. (1969). Auditory thresholds of the scombrid fish (*Euthynnus affinis*) with comments on the use of sound in tuna fishing. Fisheries and Aquaculture Report (FAO). (No. 62). FAO.
Jézéquel, Y., Jones, I. T., Bonnel, J., Chauvaud, L., Atema, J. and Mooney, A. T. (2021). Sound detection by the American lobster (*Homarus americanus*). *J. Exp. Biol.* **224**, jeb240747. doi:10.1242/jeb.240747
Kalmijn, A. J. (1988). Hydrodynamic and acoustic field detection. In *Sensory Biology of Aquatic Animals* (ed. J. Atema, R. R. Fay, A. N. Popper and W. N. Tavolga), pp. 83-130. Springer. doi:10.1007/978-1-4612-3714-3_4
Kelly, J. C. and Nelson, D. R. (1975). Hearing thresholds of the horn shark, *Heterodontus francisci*. *J. Acoust. Soc. Am.* **58**, 905-909. doi:10.1121/1.380742

Kenyon, T. N., Ladich, F. and Yan, H. Y. (1998). A comparative study of hearing ability in fishes: the auditory brainstem response approach. *J. Comp. Physiol. A* **182**, 307-318. doi:10.1007/s003590050181
Klimley, P. and Myrberg, A. A. (1979). Acoustic stimuli underlying withdrawal from a sound source by adult lemon sharks, *Negaprion Brevirostris* (Poey). *Bull. Mar. Sci.* **29**, 447-458.
Ladich, F. and Fay, R. R. (2013). Auditory evoked potential audiometry in fish. *Rev. Fish Biol. Fish.* **23**, 317-364. doi:10.1007/s11160-012-9297-z
Ladich, F. and Wysocki, L. E. (2009). Does speaker presentation affect auditory evoked potential thresholds in goldfish? *Comp. Biochem. Physiol. A: Mol. Integr. Physiol.* **154**, 341-346. doi:10.1016/j.cbpa.2009.07.004
Larsen, O. N. and Radford, C. (2018). Acoustic conditions affecting sound communication in air and underwater. In *Effects of Anthropogenic Noise on Animals* (ed. H. Slabbekoorn, R. J. Dooling, A. N. Popper and R. R. Fay), pp. 109-144. Springer. doi:10.1007/978-1-4939-8574-6_5
Lauridsen, T. B., Brandt, C. and Christensen-Dalsgaard, J. (2021). Three auditory brainstem response (ABR) methods tested and compared in two anuran species. *J. Exp. Biol.* **224**, jeb237313. doi:10.1242/jeb.237313
Lowenstein, O. E. (1971). The Labyrinth. In *Fish Physiology*, (ed. W. Hoar and D. Randall), pp. 207-240. New York and London: Elsevier. doi:10.1016/S1546-5098(08)60048-5
Lowenstein, O. E. and Roberts, T. (1950). The equilibrium function of the otolith organs of the thornback ray (*Raja clavata*). *J. Physiol.* **110**, 392-415. doi:10.1113/jphysiol.1949.sp004448
Lowenstein, O. E. and Roberts, T. (1951). The localization and analysis of the responses to vibration from the isolated elasmobranch labyrinth. A contribution to the problem of the evolution of hearing in vertebrates. *J. Physiol.* **114**, 471-489. doi:10.1113/jphysiol.1951.sp004638
Maisey, J. G. and Lane, J. A. (2010). Labyrinth morphology and the evolution of low-frequency phonoreception in elasmobranchs. *C. R. Palevol* **9**, 289-309. doi:10.1016/j.crpv.2010.07.021
Maruska, K. P. and Sisneros, J. A. (2016). Comparison of electrophysiological auditory measures in fishes. In *Fish Hearing and Bioacoustics* (ed. J. A. Sisneros), pp. 227-254. Springer. doi:10.1007/978-3-319-21059-9_11
Mickle, M. F. and Higgs, D. M. (2022). Towards a new understanding of elasmobranch hearing. *Mar. Biol.* **169**, 12. doi:10.1007/s00227-021-03996-8
Mickle, M. F., Pieniazek, R. H. and Higgs, D. M. (2020). Field assessment of behavioural responses of southern stingrays (*Hypanus americanus*) to acoustic stimuli. *R. Soc. Open Sci.* **7**, 191544. doi:10.1098/rsos.191544
Mooney, A. T., Hanlon, R. T., Christensen-Dalsgaard, J., Madsen, P. T., Ketten, D. R. and Nachtigall, P. E. (2010). Sound detection by the longfin squid (*Loligo pealeii*) studied with auditory evoked potentials: sensitivity to low-frequency particle motion and not pressure. *J. Exp. Biol.* **213**, 3748-3759. doi:10.1242/jeb.048348
Mulligan, K. P. and Gauldie, R. (1989). The biological significance of the variation in crystalline morph and habit of otoconia in elasmobranchs. *Copeia* **4**, 856-871. doi:10.2307/1445969
Myrberg, A. A. (1972). Using sound to influence the behaviour of free-ranging marine animals. In *Behavior of Marine Animals. Current Perspectives in Research Volume 2: Vertebrates* (ed. H. E. Winn and B. L. Olla), pp. 435-468. Springer. doi:10.1007/978-1-4684-0910-9_7
Myrberg, A. A., Gordon, C. R. and Klimley, P. (1976). Attraction of free ranging sharks by low frequency sound, with comments on its biological significance. In *Sound Reception in Fish* (ed. A. Schuijf and A. D. Hawkins), pp. 205-228. Amsterdam: Elsevier.
Myrberg, A. A., Gordon, C. R. and Klimley, P. (1978). Rapid withdrawal from a sound source by open–ocean sharks. *J. Acoust. Soc. Am.* **64**, 1289-1297. doi:10.1121/1.382114
Nachtigall, P. E., Supin, A. Y., Pawloski, J. and Au, W. W. (2004). Temporary threshold shifts after noise exposure in the bottlenose dolphin (*Tursiops truncatus*) measured using evoked auditory potentials. *Mar. Mamm. Sci.* **20**, 673-687. doi:10.1111/j.1748-7692.2004.tb01187.x
Nachtigall, P. E., Mooney, A. T., Taylor, K. A. and Yuen, M. M. (2007). Hearing and auditory evoked potential methods applied to odontocete cetaceans. *Aquat. Mamm.* **33**, 6. doi:10.1578/AM.33.1.2007.6
Nedelec, S. L., Campbell, J., Radford, A. N., Simpson, S. D. and Merchant, N. D. (2016). Particle motion: the missing link in underwater acoustic ecology. *Methods Ecol. Evol.* **7**, 836-842. doi:10.1111/2041-210X.12544
Nelson, D. R. (1967). Hearing thresholds, frequency discrimination, and acoustic orientation in the lemon shark, *Negaprion brevirostris* (Poey). *Bull. Mar. Sci.* **17**, 741-768.
Nelson, D. R. and Gruber, S. H. (1963). Sharks: attraction by low-frequency sounds. *Science* **142**, 975-977. doi:10.1126/science.142.3594.975
Nelson, D. R. and Johnson, R. H. (1972). Acoustic attraction of Pacific reef sharks: Effect of pulse intermittency and variability. *Comp. Biochem. Physiol. A Physiol.* **42**, 85-95. doi:10.1016/0300-9629(72)90370-2
Parmentier, E., Banse, M., Boistel, R., Compère, P., Bertucci, F. and Colleye, O. (2020). The development of hearing abilities in the shark *Scyliorhinus canicula*. *J. Anat.* **237**, 468-477. doi:10.1111/joa.13212
Parvulescu, A. (1964). Problems of propagation and processing. In *Marine Bioacoustics* (ed. W. N. Tavolga), pp. 87-100). Pergamon Press.
Popper, A. N. and Fay, R. R. (1977). Structure and function of the elasmobranch auditory system. *Am. Zool.* **17**, 443-452. doi:10.1093/icb/17.2.443
Popper, A. N. and Fay, R. R. (2011). Rethinking sound detection by fishes. *Hear. Res.* **273**, 25-36. doi:10.1016/j.heares.2009.12.023
Popper, A. N. and Hawkins, A. D. (2021). Fish hearing and how it is best determined. *ICES J. Mar. Sci.* **78**, 2325-2336. doi:10.1093/icesjms/fsab115
Popper, A. N., Hawkins, A. D., Sand, O. and Sisneros, J. A. (2019). Examining the hearing abilities of fishes. *J. Acoust. Soc. Am.* **146**, 948-955. doi:10.1121/1.5120185
Popper, A. N., Hawkins, A. D. and Sisneros, J. A. (2021). Fish hearing "Specialization"–A re-evaluation. *Hear. Res.* **425**, 108393. doi:10.1016/j.heares.2021.108393
Radford, C. A., Montgomery, J. C., Caiger, P. and Higgs, D. (2012). Pressure and particle motion detection thresholds in fish: a re-examination of salient auditory cues in teleosts. *J. Exp. Biol.* **215**, 3429-3435. doi:10.1242/jeb.073320
Retzius, G. (1881). *Das Gehörorgan der Fische und Amphibien.* Samson & Wallin.
Richard, J. D. (1968). Fish attraction with pulsed low-frequency sound. *J. Fish. Board Canada* **25**, 1441-1452. doi:10.1139/f68-125
Rogers, P. H. and Cox, M. (1988). Underwater sound as a biological stimulus. In *Sensory Biology of Aquatic Animals*, (ed. J. Atema, R. R. Fay, A. N. Popper and W. N. Tavolga), pp. 131-149. Springer. doi:10.1007/978-1-4612-3714-3_5
Rogers, P. H., Hawkins, A. D., Popper, A. N., Fay, R. R. and Gray, M. D. (2016). Parvulescu revisited: small tank acoustics for bioacousticians. In *The Effects of Noise on Aquatic Life II*, (ed. A. N. Popper and A. Hawkins), pp. 933-941. Springer. doi:10.1007/978-1-4939-2981-8_115
Sand, O. and Enger, P. S. (1973). Evidence for an auditory function of the swimbladder in the cod. *J. Exp. Biol.* **59**, 405-414. doi:10.1242/jeb.59.2.405
Sauer, D. J., Yopak, K. E. and Radford, C. A. (2022). Ontogeny of the inner ear maculae in school sharks (*Galeorhinus galeus*). *Hear. Res.* **424**, 108600. doi:10.1016/j.heares.2022.108600
Sisneros, J. A., Popper, A. N., Hawkins, A. D. and Fay, R. R. (2016). Auditory evoked potential audiograms compared with behavioral audiograms in aquatic animals. In *The effects of noise on aquatic life II*, (ed. A. N. Popper and A. D. Hawkins), pp. 1049-1056. Springer. doi:10.1007/978-1-4939-2981-8_130
Tester, A. L., Kendall, J. I. and Milisen, W. B. (1972). Morphology of the ear of the shark genus *Carcharhinus*, with particular reference to the macula neglecta. *Pac. Sci.* **26**, 264-274.
Vetter, B. J., Brey, M. K. and Mensinger, A. F. (2018). Reexamining the frequency range of hearing in silver (*Hypophthalmichthys molitrix*) and bighead (*H. nobilis*) carp. *PLoS One* **13**, e0192561. doi:10.1371/journal.pone.0192561
Vetter, B. J., Seeley, L. H. and Sisneros, J. A. (2019). Lagenar potentials of the vocal plainfin midshipman fish, *Porichthys notatus*. *J. Comp. Physiol. A* **205**, 163-175. doi:10.1007/s00359-018-01314-0
Wiernicki, C. J., Liang, D., Bailey, H. and Secor, D. H. (2020). The effect of swim bladder presence and morphology on sound frequency detection for fishes. *Rev. Fish. Sci. Aquac.* **28**, 459-477. doi:10.1080/23308249.2020.1762536
Wysocki, L. E., Codarin, A., Ladich, F. and Picciulin, M. (2009a). Sound pressure and particle acceleration audiograms in three marine fish species from the Adriatic Sea. *J. Acoust. Soc. Am.* **126**, 2100-2107. doi:10.1121/1.3203562
Wysocki, L. E., Montey, K. and Popper, A. N. (2009b). The influence of ambient temperature and thermal acclimation on hearing in a eurythermal and a stenothermal otophysan fish. *J. Exp. Biol.* **212**, 3091-3099. doi:10.1242/jeb.033274
Xiao, J. and Braun, C. B. (2008). Objective threshold estimation and measurement of the residual background noise in auditory evoked potentials of goldfish. *J. Acoust. Soc. Am.* **124**, 3053-3063. doi:10.1121/1.2982366
Yan, H. Y., Anraku, K. and Babaran, R. P. (2010). Hearing in marine fish and its application in fisheries. In *Behavior of Marine Fishes: Capture Processes and Conservation Challenges* (ed. P. He), pp. 45-64. Wiley–Blackwell. doi:10.1002/9780813810966.ch3